

Supplementary Materials for

Thermally assisted nanotransfer printing with sub–20-nm resolution and 8-inch wafer scalability

Tae Wan Park, Myunghwan Byun, Hyunsung Jung, Gyu Rac Lee, Jae Hong Park, Hyun-Ik Jang, Jung Woo Lee, Se Hun Kwon, Seungbum Hong, Jong-Heun Lee, Yeon Sik Jung*, Kwang Ho Kim*, Woon Ik Park*

*Corresponding author. Email: ysjung@kaist.ac.kr (Y.S.J); kwhokim@pusan.ac.kr (K.H.K); thane0428@pknu.ac.kr (W.I.P)

Published 29 July 2020, *Sci. Adv.* **6**, eabb6462 (2020)
DOI: 10.1126/sciadv.abb6462

The PDF file includes:

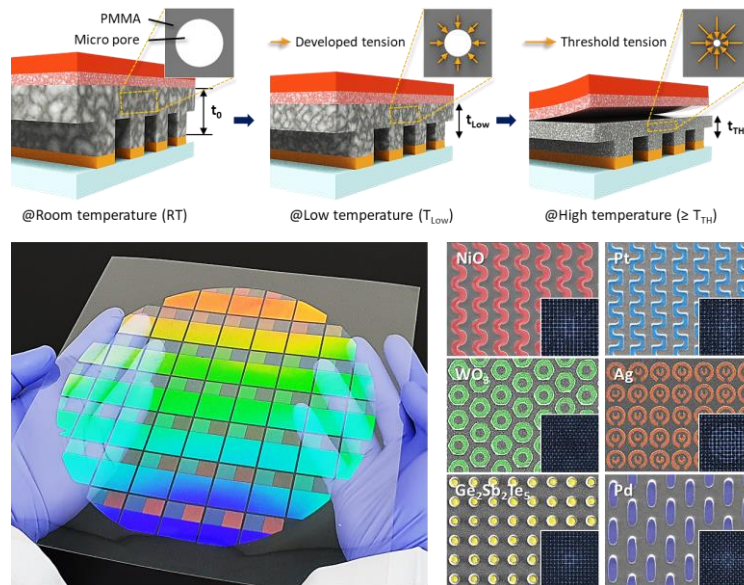
Figs. S1 to S12
Legend for movie S1

Other Supplementary Material for this manuscript includes the following:

(available at advances.sciencemag.org/cgi/content/full/6/31/eabb6462/DC1)

Movie S1

Table of Contents Graphic



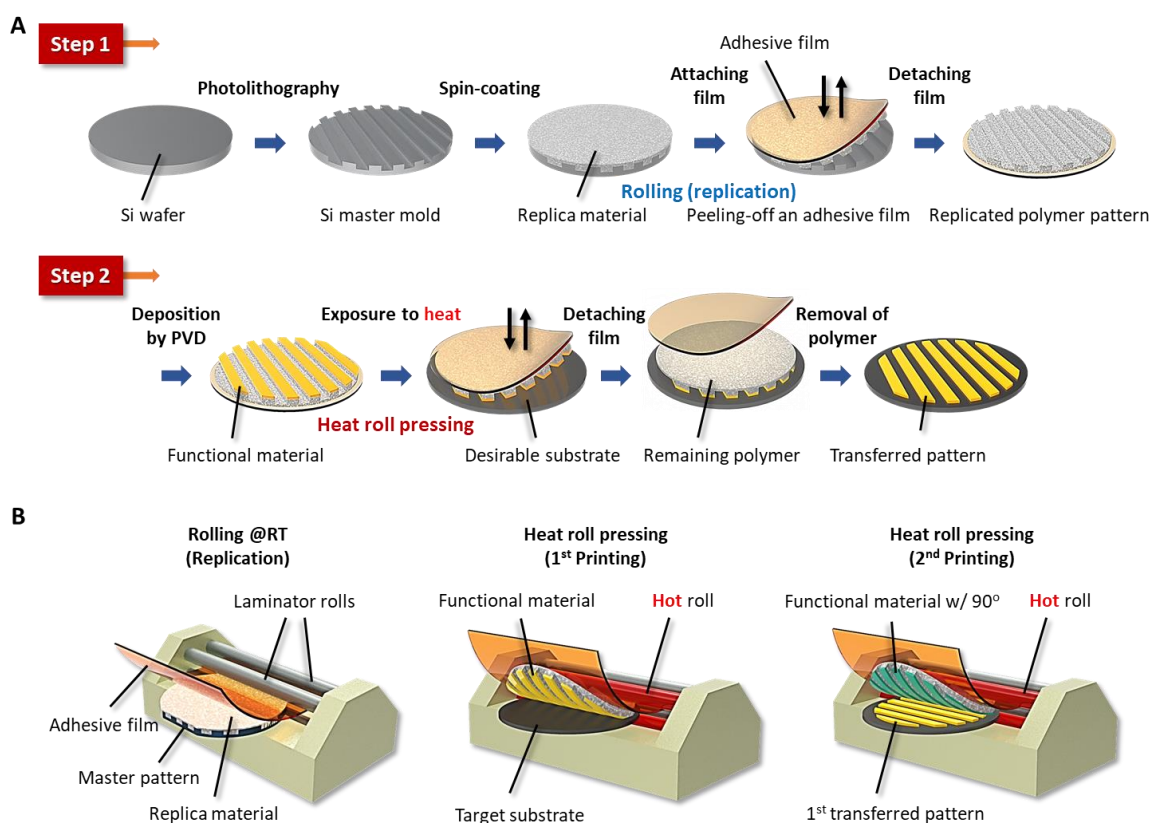


Fig. S1. Procedure of the T-nTP process at 8-inch wafer scale. (A) (Step 1) Pattern replication. The polymer replica material is spin-coated onto the 8-inch Si master mold fabricated by a photolithography process. The surface-patterned polymeric replica film is formed by peeling-off the spin-coated polymeric material on the Si master mold using an adhesive polyimide (PI) film. During the replication process, uniform surface contact and pressure between the PI film and the polymer film is of paramount importance for large-area patterning. (Step 2) Transfer printing of a functional structure. The functional materials are formed on the surface of a replicated polymer pattern by physical vapor deposition (PVD). Subsequently, the functional nanostructure on the replica pattern is transfer-printed onto the target substrates at 8-inch wafer scale via a short (≤ 20 sec) contact and release process using a heat rolling press system capable of supplying uniform pressure and heat. The appropriately applied heat in this case weakens the adhesion between the adhesive film and the polymeric replica pattern, allowing the functional nanostructures onto the polymer replica pattern to be transfer-printed on the substrates. The functional nanopatterns on the substrate are finally obtained after solvent-removing the residual polymer replica film used as a medium for the pattern transfer step. (B) T-nTP processes at 8-inch wafer by laminator.

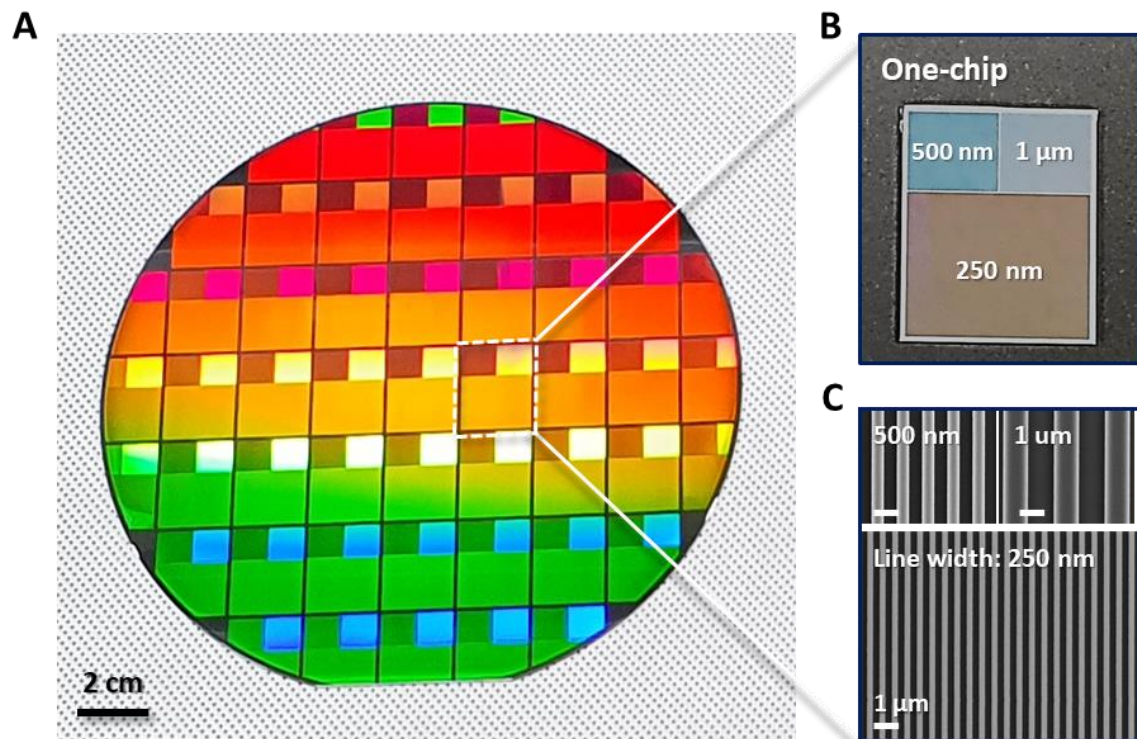


Fig. S2. 8-inch Si master mold fabricated by photolithography. (A) The 8-inch Si master mold consists of approximately 50 chips. (B) A single chip. (C) Top-view SEM images of (B). Each chip is composed of three different line/space patterns with widths of 250/250 nm (bottom), 500/500 nm (top, left), and 1/1 μm (top, right). Photo credit: T. W. Park (KICET and Korea University).

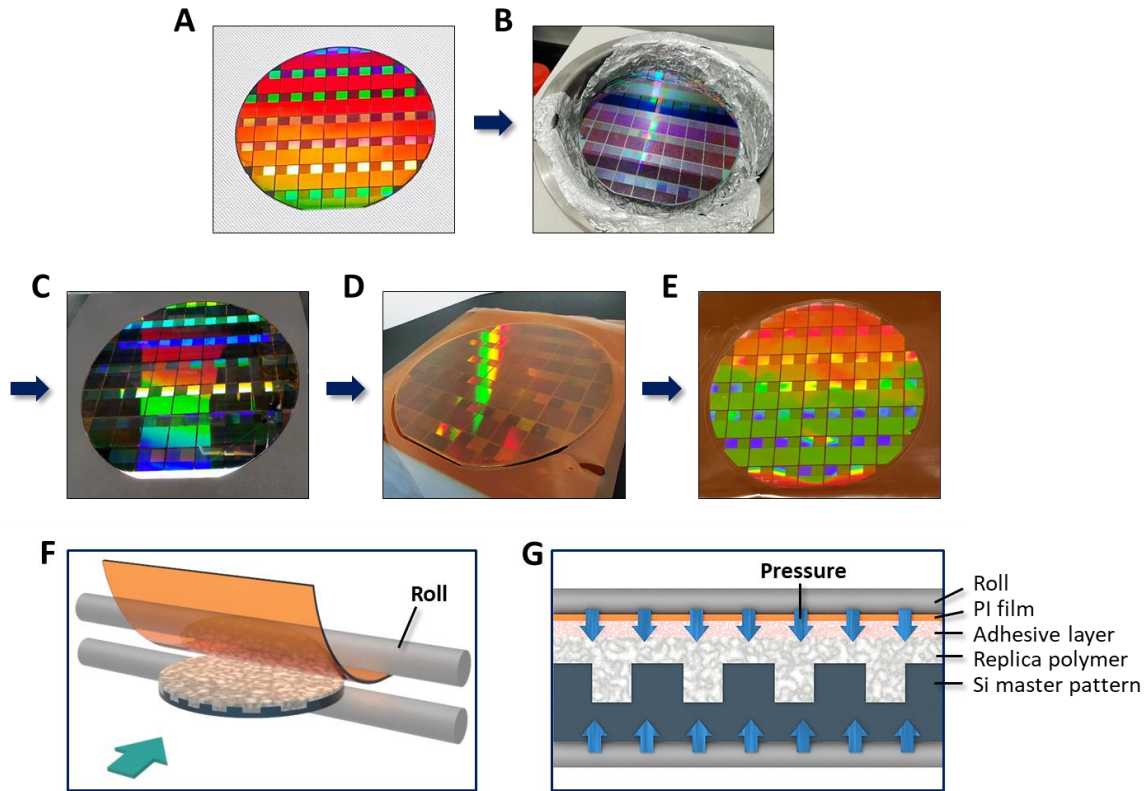


Fig. S3. Pattern replication process at 8-inch wafer scale. (A) 8-inch Si master mold. (B) Spin-coating of the replica material (PMMA). (C) PMMA-coated Si master mold, (D) After attaching the PI adhesive film onto the PMMA thin film. (E) Duplicated 8-inch PMMA replica pattern after the detachment of the PI film. (F) Replication process using a rolling press system at RT. (G) Cross-sectional schematic of the replication process, which provides uniform pressure when the sample is passed between the two rolls. To fabricate the 8-inch polymer replica, uniform pressure over the entire surface is required. Photo credit: T. W. Park (KICET and Korea University).

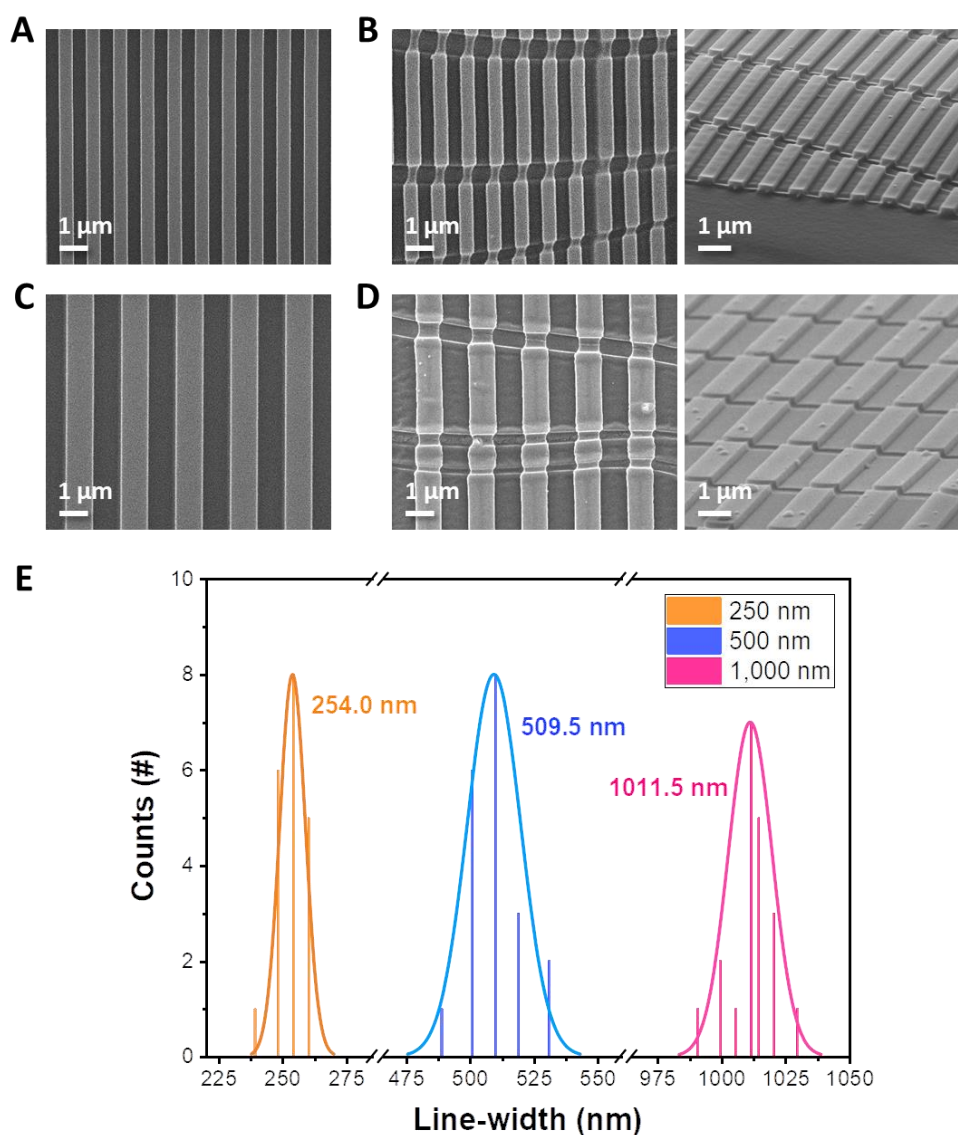


Fig. S4. Comparison of the rolling process and a manual process for the replicated PMMA pattern. (A & C) Rolling press system. (B & D) Manual process done by hand. (A & B) Line width: 500 nm. (C & D) Line width: 1 μm. Well-defined PMMA replica patterns were obtained when using the rolling press system, while defective replica patterns with many microcracks and distortions were formed by the manual process. (E) The distribution of line widths of 250 nm, 500 nm, and 1 μm displays excellent pattern uniformity, showing mean line width values of 254 nm, 509.5 nm, and 1011.5 nm, respectively. The error range is less than 1.9%.

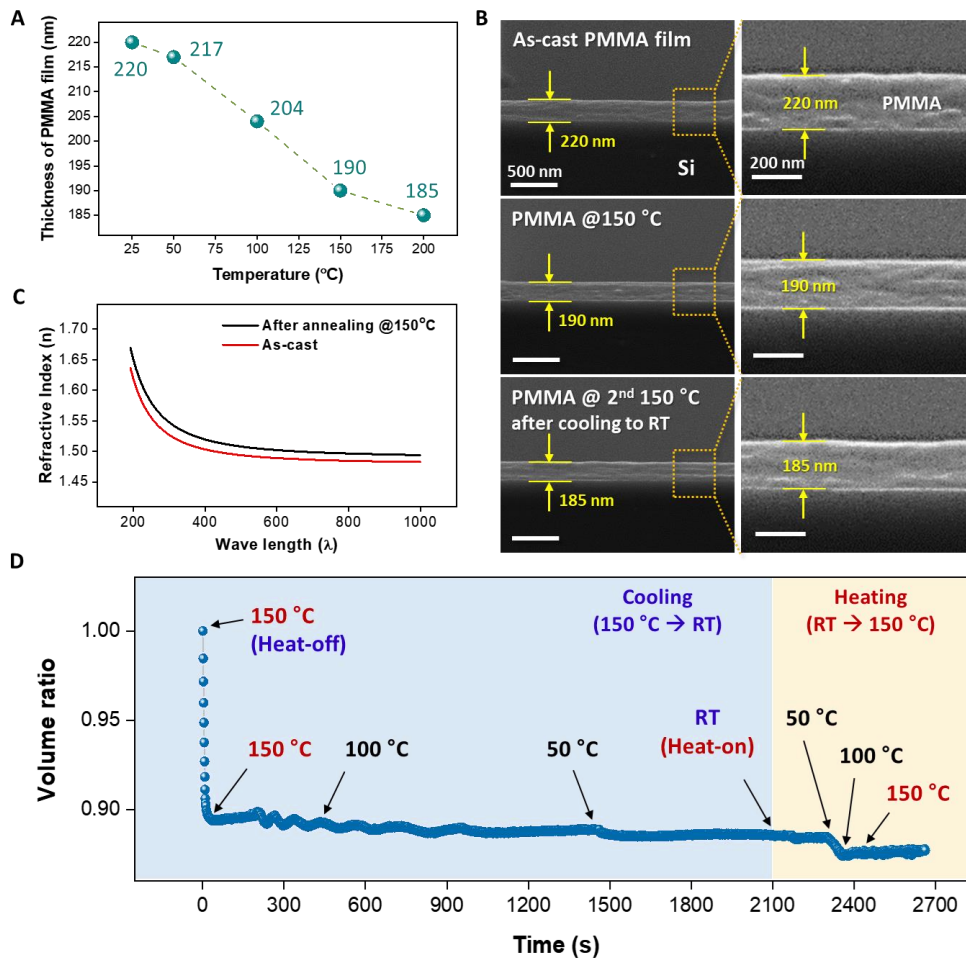


Fig. S5. Temperature dependency on the volume change of the PMMA thin film. (A) Graph of PMMA film thickness depending on the annealing temperature. (B) Comparison of refractive indexes of PMMA thin film before and after annealing at 150 °C. (C) Cross-sectional SEM images for PMMA film shrinkage when annealed at 150 °C, and re-annealed at 150 °C after cooling to RT, compared to the as-cast PMMA thin film. (D) Volume ratio of PMMA thin film when cooling down from 150 °C to RT and re-heating to 150 °C. The volume ratio was measured by optical reflectometry. After stopping the heat treatment at 150 °C, the reduced thickness of the PMMA film did not recover to its initial thickness, even after 35 minutes. While the initial thickness was about 220 nm, the thickness was decreased to 190 nm at 150 °C. Furthermore, when the PMMA film cooled to RT was annealed to 150 °C again, the contracted PMMA film was slightly further reduced rather than recovered to the initial thickness.

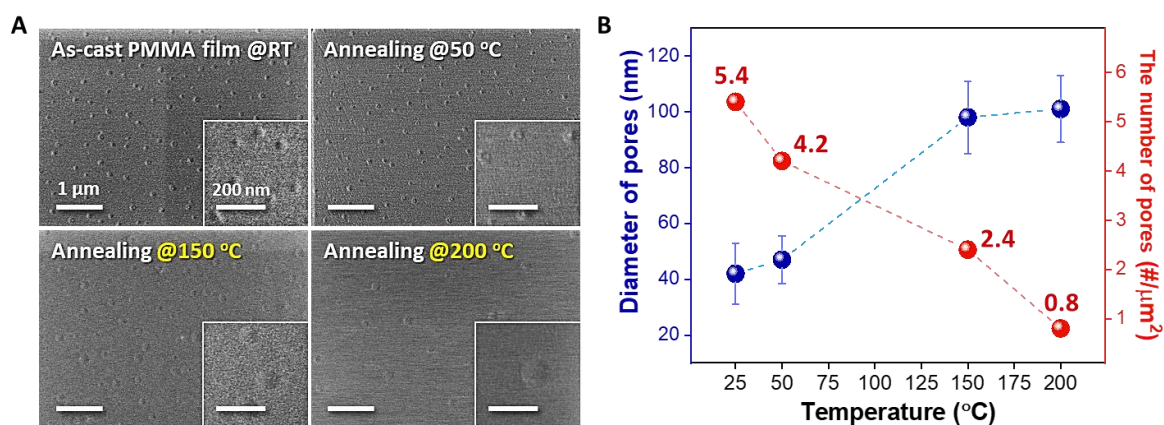


Fig. S6. Temperature dependency on the size and number of pores on the PMMA surfaces.

(A) Top-view SEM images of PMMA surfaces at various annealing temperatures. (B) Diameters and numbers of pores depending on the temperature. The number of nanoscale pores with a diameter of ~ 40 nm on the as-cast PMMA thin film decreases as temperature increases, showing an increase of pore size to ~ 100 nm at 150 °C.

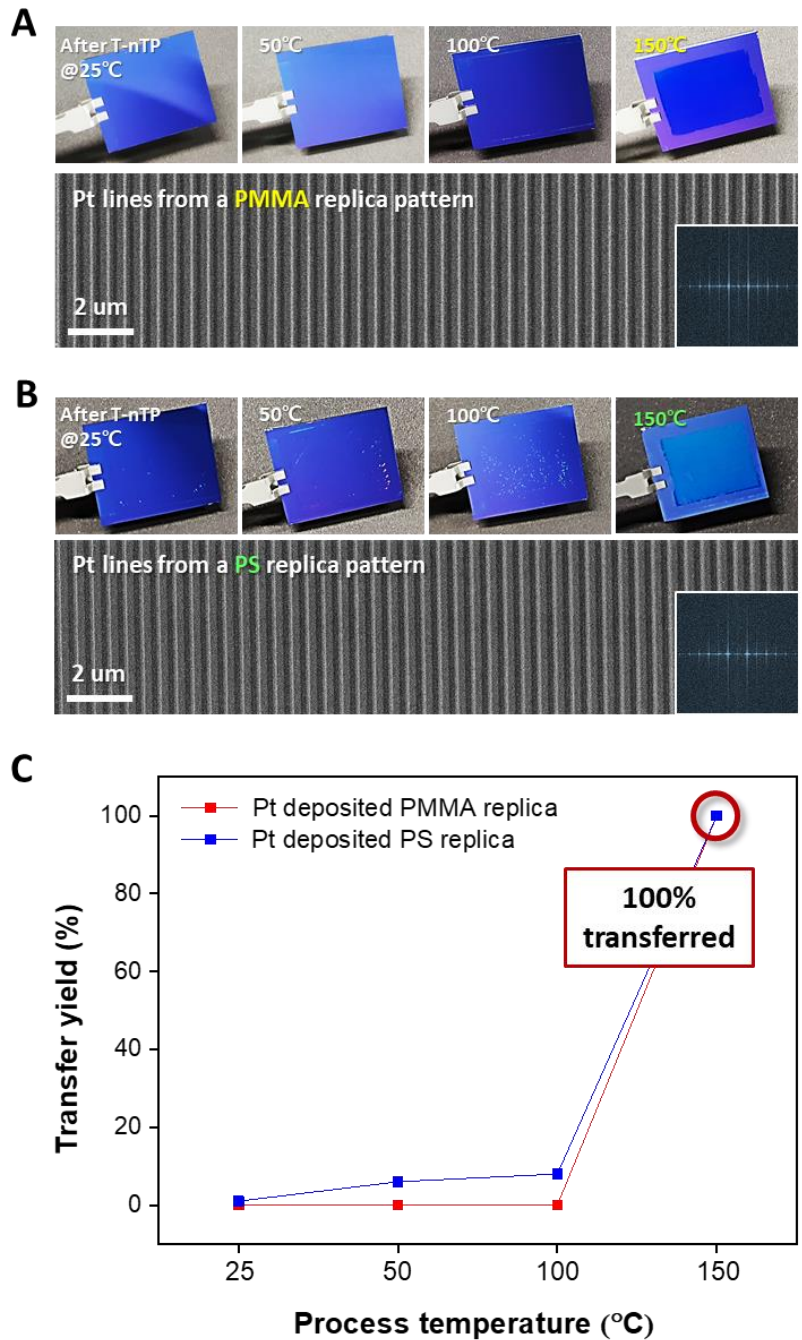


Fig. S7. Temperature dependency on the yield during the T-nTP process. Photographs and SEM images show the transfer yield or transferability after the printing of 250 nm Pt line patterns on SiO₂/Si substrate at various temperatures when using (A) PMMA and (B) PS replica materials. (C) Graph of the dependency on the printing temperature. Both the PMMA and PS replica materials show excellent transfer yield of 100% at 150 °C. Photo credit: T. W. Park (KICET and Korea University).

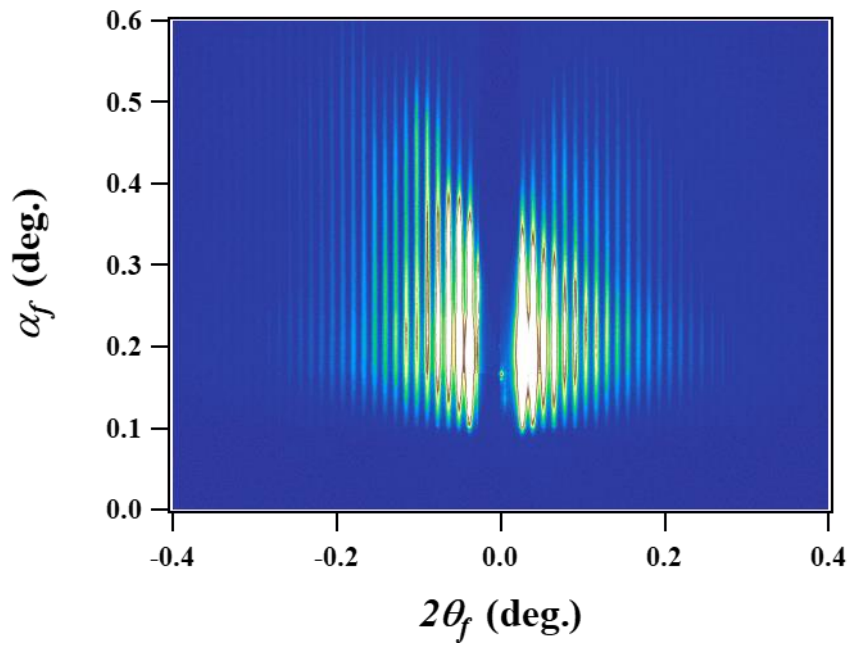


Fig. S8. Grazing-incidence small-angle X-ray scattering (GISAXS) measurement result of Pt nanowires. The GISAXS measurement was conducted with the transfer-printed Pt nanowires with a width of 250 nm at the center of the 8-inch PET substrate. The consistent peaks suggest the excellent pattern uniformity of the nanowires.

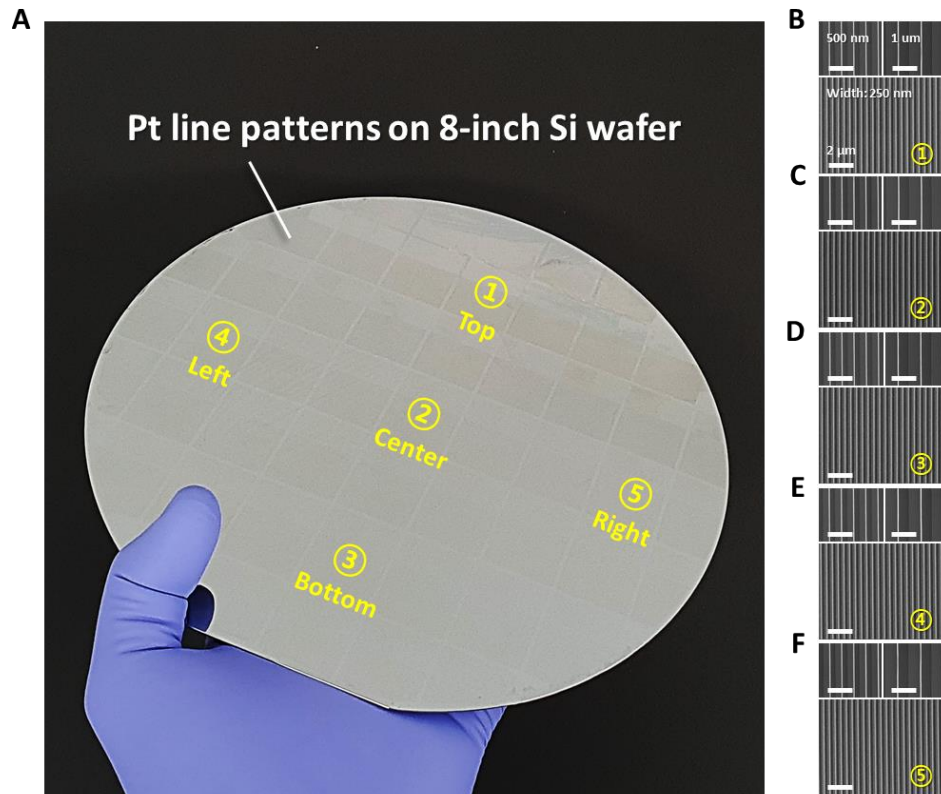


Fig. S9. Transfer-printed micro- and nanowires at 8-inch Si wafer via T-nTP. (A) Photographic image of the transfer-printed Pt nanowires on the 8-inch Si wafer. Photo credit: T. W. Park (KICET and Korea University). **(B-F)** SEM images of the Pt micro- and nanowires at five points (top, center, bottom, left, and right) on the Si wafer.

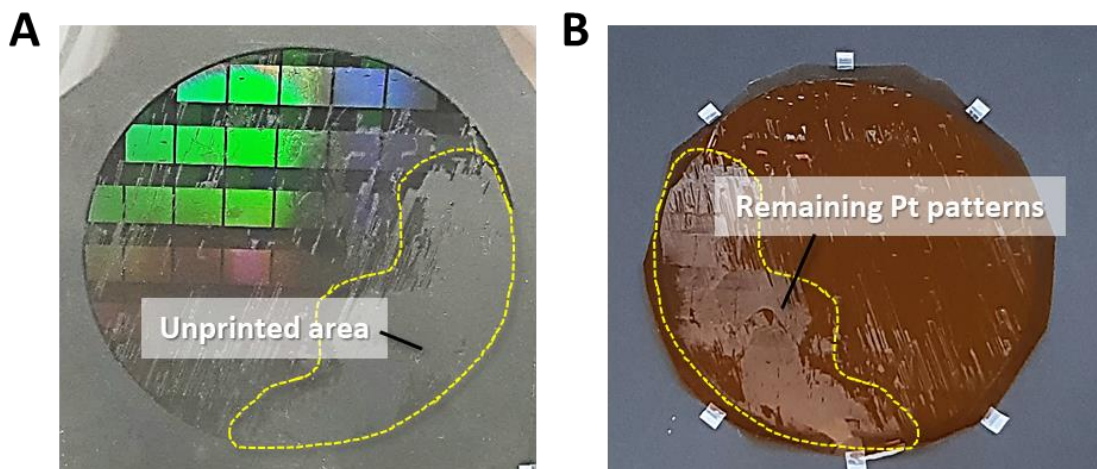


Fig. S10. Transfer-printed patterns at 8-inch scale via the S-nTP process. (A) Photograph image of the printed patterns on the PET substrate via S-nTP using a roll-pressing system. **(B)** Photographic image of the 8-inch replica pattern after transfer printing by S-nTP. Photo credit: T. W. Park (KICET and Korea University).

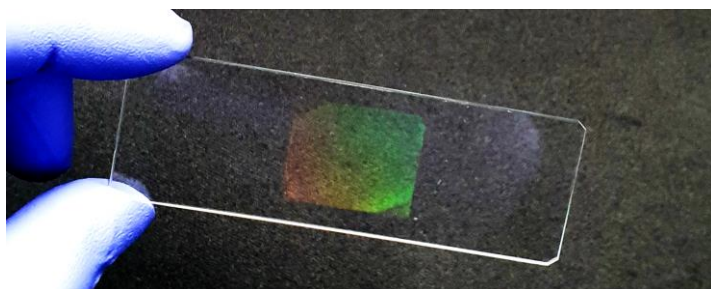


Fig. S11. Transfer-printed pattern on the slippery surface. Photograph image of the transfer-printed line pattern with a width of 250 nm on the slide glass substrate. Photo credit: T. W. Park (KICET and Korea University).

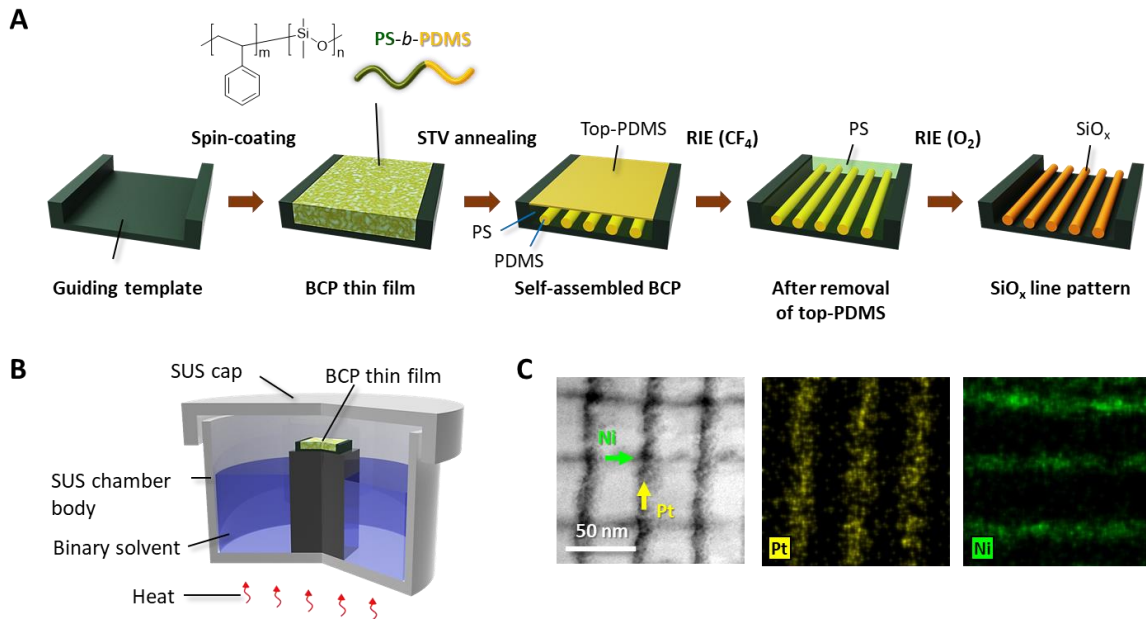


Fig. S12. Procedure for the pattern formation of the SiO_x line structure by the DSA of SD45 BCP. (A) DSA process for the self-assembled SiO_x line structure from SD45 BCP. (B) Schematic illustration of the solvothermal annealing step. Cylinder-forming PS-*b*-PDMS BCP was spin-coated onto a Si guiding template fabricated by photolithography. The BCP thin film was then annealed with a binary-solvent of toluene and heptane (mixing ratio of the binary solvent, $V_{\text{Tol}}/V_{\text{Hep}} = 1$) at 65 °C followed by etched with CF_4 and O_2 plasma through an RIE system to remove the top-PDMS layer and PS matrix, respectively. (C) Bright-field TEM image and EDS elemental mapping images of a NiO_x/Pt cross-bar array with a line width of 14 nm.

Movie S1. Thermally assisted nanotransfer printing (T-nTP) process.